Polymers as Fuel for Laser Plasma Thrusters
A correlation of thrust with material and plasma properties by mass spectrometry

Lukas Urech[a], Thomas Lippert*[a], Claude R. Phipps[b], Alexander Wokaun[a]
[a]General Energy Department, Paul Scherrer Institut, 5232 Villigen PSI Switzerland
[b]Photonic Associates LLC, Santa Fe, NM 87508, USA

ABSTRACT

The micro laser plasma thruster (μLPT) is a micro propulsion device, designed for the steering and propelling of small satellites (1 to 10 kg). A laser is focused onto a polymer layer on a substrate to form a plasma. The thrust produced by this plasma is used to control the satellite motion.
To understand the influence of the specific properties of the polymers, three different "high"- and "low"-energetic polymers were tested: poly(vinyl chloride) (PVC) as a low-energetic reference polymer that showed the best properties among commercial polymers, a glycidyl azide polymer (GAP), and poly(vinyl nitrate) (PVN) as high-energetic polymers. It was necessary to dope the polymers with carbon nanoparticles or an IR-dye to achieve absorption at the irradiation wavelength in the near IR.

Decomposition into smaller fragmentation was measured for the energetic polymers than for PVC corresponding well to the higher momentum coupling coefficient of the energetic polymers, which indicates that more thrust can be gained from a chosen incident laser power.

The measurements of the kinetic energies of selected decomposition fragments revealed no significant difference between the different carbon doped polymers. Only for GAP with the IR-dye a change in the ratio between ions with different kinetic energy was observed with increasing fluence. More C^+ ions with higher kinetic energy were detected at higher fluences. No correlation between the kinetic energies of the ablation products and the specific impulse could be established for the obtained data.

Keywords: Laser plasma thruster, polymer, mass spectrometry, thrust

1. INTRODUCTION

The micro laser plasma thruster (μ-LPT) is a micro propulsion device designed for the steering and propelling of small satellites (1 to 10 kg). The requirements for a propulsion system for such small satellites are low mass, volume and power consumption. To control bidirectional thrust on three axes, six thrust units are needed. For a 25-kg satellite, a low weight of these propulsion devices (less than one kg) is therefore the most important criterion. Other requirements are at least 75 μN thrust and 300 N-s lifetime impulse [1, 2]. The laser plasma thruster can meet all requirements, as it takes advantage of the predictable physics of the plasma formation in laser-material interaction. The confining force involved in the plasma formation, also make it possible that no nozzle is required to control the jet.

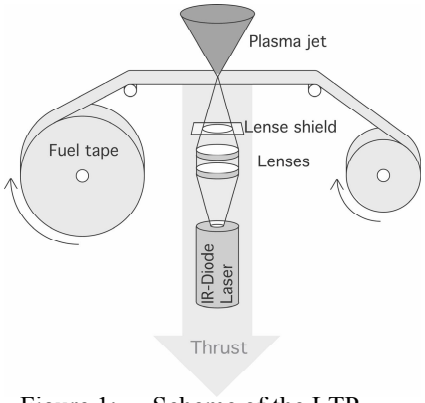

Figure 1: Scheme of the LTP.

* thomas.lippert@psi.ch; phone +41 56 310 4076; fax +41 56 310 2688

High-Power Laser Ablation VI, edited by Claude R. Phipps, Proc. of SPIE
Vol. 6261, 626114, (2006) · 0277-786X/06/$15 · doi: 10.1117/12.672776

Due to the specific demands (weight and power), the μ-LPT is driven by small powerful diode lasers, which emit in the near IR (920-980 nm) with an available power of 1 to 15 W and a pulse length from 100 μs to the millisecond range [3]. This pulse duration and wavelength require the utilization of materials for the fuel with low thermal conductivity, i.e. polymers [4, 5].

The functional principle of a μLPT is shown in Fig 1. A laser is focused on to a polymer layer on a substrate to form a plasma. The thrust produced by this plasma is used to control the satellite motion. The tape design allows an easy fuel supply and a high usage of the fuel.
The transparent support layer also protects the optics and the laser from contamination by ablation products, as it builds a physical barrier between the plasma and the lens. The support layer also needs to meet special requirements, such as transparency in the near IR, flexibility and resistance to solvents used for the fuel layer polymer. Different polymers such as cellulose acetate, poly(ethylene terephthalate), fluorinated ethylene-propylene and Kapton™ have been tested. Kapton™ has been selected as substrate, due to its solvent resistance, physical toughness and outgasing properties [1, 6].

2. EXPERIMENTAL

To understand the influence of the martial properties of the used fuel-layer polymer, three different polymers were investigated. Poly(vinyl chloride) (PVC, obtained from Aldrich) was used as a commercial available and well studied reference, which showed good results in previous tests [7, 8]. A Glycidyl acide polymer POLYOL (GAP, obtained from Nitrochemie, Wimmis) and Poly(vinyl nitrate) (PVN, synthesized according to [9]) were used as "high"-energetic polymers (chemical structures shown in Fig. 2). These energetic polymers release high amounts of chemically stored energy when they are decomposed. In Table 1 the decomposition enthalpy and the decomposition temperature for all three polymers are shown.

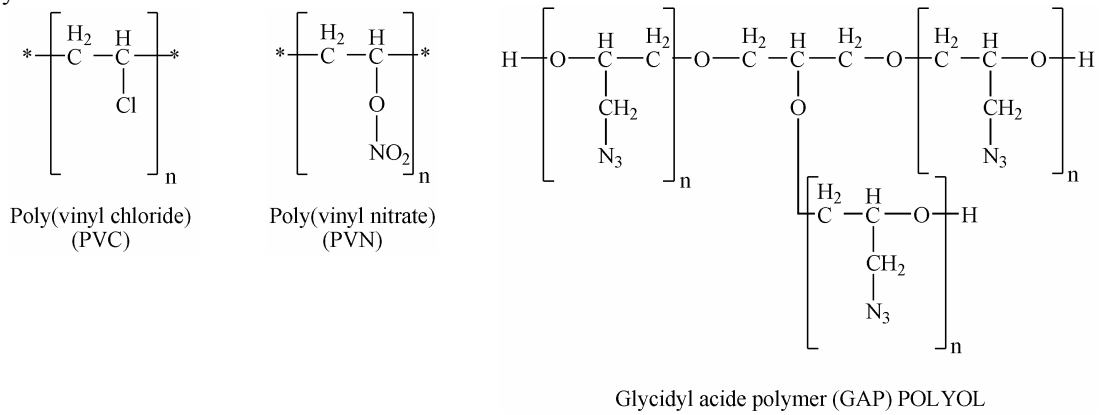

Figure 2: Chemical Structure of PVC, PVN and GAP POLYOL

As the polymers used do not absorb in the near IR, absorbers had to be added. For all polymers carbon nanoparticles (Carbon nanopearls 2000 (Cabot) for PVC and GAP and basic carbon nanoparticles for PVN) and in the case of GAP also an IR-dye (Epolite 2057 (Epoline INC.)) were used. Requirements on their properties are compatibility with the applied polymer-solvent systems (see Table 1) and stability over time.

Table 1.: Solvents used for solvent casting GAP, PVN and PVC and the decomposition properties of the three polymers.

Polymer	Solvent	Decomposition Temperature [°C]	Decomposition* Enthalpy [J/g]
GAP	Ethyl acetate	249	-2053
PVN	Acetone	204	-3829
PVC	Cyclohexanone	241,288,383	-418

*measured by DSC, using carbon doped samples of the polymer.

The main difference between the two different absorbers is the distribution within the polymer which lead to different decomposition behaviors [8]. The carbon is present in the form of nanoparticles of 15 nm diameter and agglomerates of up to 15 µm diameter [10], whereas the IR-dye is distributed on a molecular level. All polymer-absorber systems were prepared as described in [8].
The polymers will be referred to in this paper with the abbreviation of the polymer and by indicating the dopant by "+ C" for carbon and "+ IR" for IR-dye.

2.1. Mass spectrometry measurements

For the mass spectrometry measurements the fundamental wavelength (λ=1064nm) of a Nd:YAG (Brilliant B Nd:YAG, Quantel, τ= 6 ns) with a Super-Gaussian beam profile including some hotspots was utilized to ablate the polymer. All mass spectrometry measurements have been performed at room temperature and a pressure of $1*10^{-7}$ mbar.

All mass spectrometric measurements have been performed in a UHV chamber with a Electrostatic Quadrupole Plasma (EPQ) Analyser (Series 1000) from Hiden Analytical which allows to measure masses in the plasma, which is very dense compared to vacuum conditions normally necessary for mass spectrometric measurements.. The measurement chamber is equipped with a double load-lock, which ensures a high vacuum and short pumping times after the sample transfer.
The sample was mounted on a x-y-z translation stage and placed in the chamber with its surface normal directed at the mass spectrometer (MS). The distance between the sample and the nozzle of the MS can be varied by moving the MS. The pulsed laser beam is aimed at the surface in a 45° angle. The resulting plasma expands perpendicular to the sample surface towards the MS. Due to the limited space on a single polymer sample and the relatively high fluences used to produce a plasma only a limited number of ablation spots per sample were available. A special experimental setup (see Fig. 3) was used, to optimize the usage of the sample and to optimize the measurement signal.
A pulse generator sends a trigger signal (①) to the MS, but is blocked when the laser-shutter is closed to inhibit a triggering of the MS while the sample is moving. After a set delay to the MS trigger, a second signal (②) is sent to the Flashlamp of the Nd:YAG laser. A photodiode is then used to record the timing of the laser pulse (③) with an oscilloscope. The time span between the trigger signal for the MS and the laser pulse is referred to as "pulse delay", the length of the MS trigger signal is the "pulse width". The pulse delay is necessary to ensure that all species have been recorded. Normally a 10 µs pulse delay has been used with a 10 ms gate width.
For all polymers, the produced uncharged fragments, the positively charged ions (+ions) and the kinetic energy of the +ions for selected masses have been recorded.

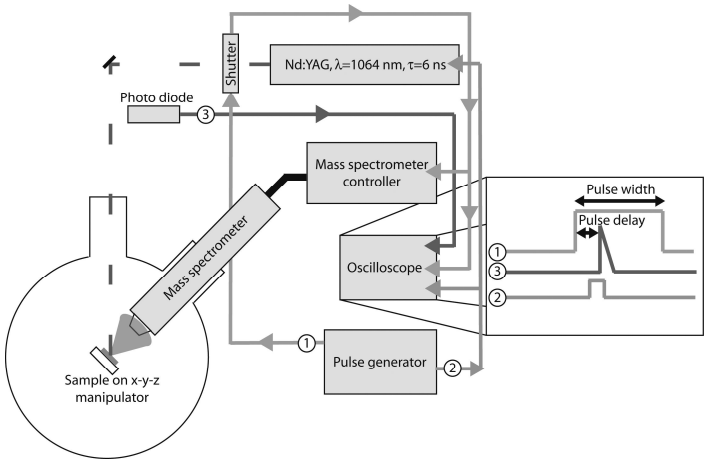

Figure 3: Mass spectrometry setup. The mass spectrometer externally triggered by a pulse generator before the laser pulse ("Pulse delay") for "Pulse width".

2.2. Thrust measurements

The target momentum of the polymers was measured with a torsion balance as described in [7] to analyze their performance in a µ-LPT. The target momentum was then used to calculate the momentum coupling coefficient C_m:

$$C_m = \frac{m\Delta v}{W} = \frac{F}{P} \qquad \text{[dyn/W]} \qquad (1)$$

where $m\Delta v$ is the target momentum produced during the laser ablation through the ejection of material. W is the induced laser pulse energy. F is the thrust, and P the incident power. The second important parameter for thrusters is the specific impulse I_{sp}, which is defined as:

$$I_{sp}g = v_E = C_m Q^* \qquad \text{[cm/s]} \qquad (2)$$

Q^* is the specific ablation energy (incident power/mass ablation rate), v_E is the exhaust velocity, and g is the acceleration due to gravity.

3. RESULTS AND DISCUSSION

3.1. Mass spectrometry

3.1.1. PVC doped with carbon nanoparticles

In Fig. 4, the mass spectrum of neutral fragments of PVC+C after irradiation at 1064 nm with a fluence of 10 J cm^{-2} is shown. This fluence is well above the plasma threshold fluence of ~6 J cm^{-2}. The main decomposition fragments can be assigned to Cl and HCl and to fragments from the polymer backbone that have also been observed for thermal degradation of PVC [11-13].

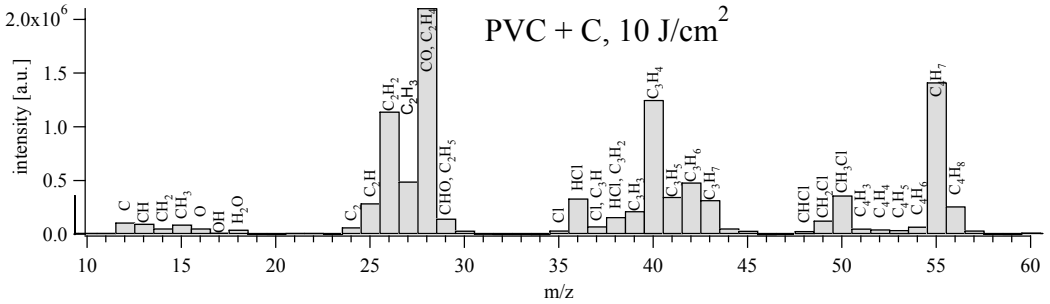

Figure 4: Mass spectrum of the neutral fragments from PVC + C after irradiation with 10 J cm^{-2} at 1064 nm.

All major peaks above 50 amu can be assigned to cyclohexanone [14], that was used as solvent for PVC [8].
The most intense positive ion signal (see Fig. 5) at mass 12 can be assigned to C^+ from the dopant (carbon), the solvent, and the polymer backbone. The main decomposition products of the polymer, i.e. Cl and HCl and small fragments from the polymer backbone are also present.

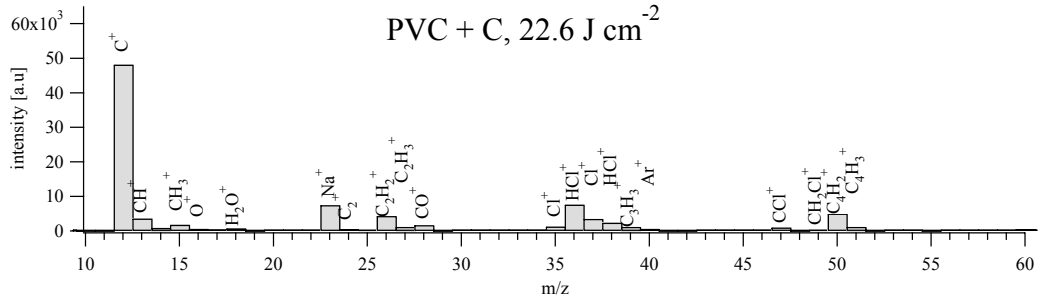

Figure 5: Mass spectrum of the positive charged ion fragments from PVC + C after irradiation with 23 J cm^{-2} at 1064 nm

The energy distribution of C^+ for different fluences is shown in Fig. 6. For all applied laser fluences, ions with the same kinetic energies can be detected at 10 eV, 40 eV and at 60 eV. At 7 J/cm^2, the majority of the C^+-ions have an energy of 60 eV. At 14 J/cm^2, the peak 40 eV has the highest intensity, and at 23 J/cm^2, the peaks at 10 and 40 eV are dominant. The total counts also increase with increasing intensity.

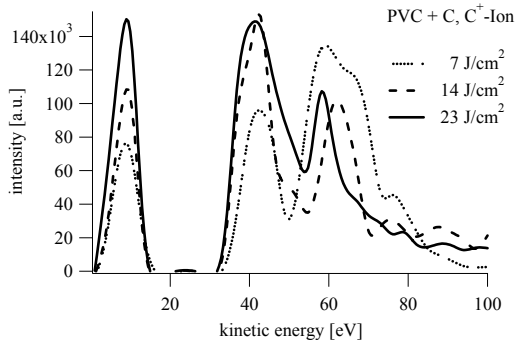

Figure 6: Kinetic energy C^+ of PVC+C for different irradiation fluences with 1064 nm

3.1.2. GAP doped with carbon nanoparticles and IR-dye

The neutral mass spectra for GAP+C and GAP+IR are shown in Fig. 7. For both dopants the same fragments were detected, but with different intensities. The strongest peak in the spectra of carbon doped GAP can be assigned to HCN (m/w = 27), whereas the IR-dye doped GAP seems to decompose mainly into N_2. A weak C_2 signal can only be detected for GAP+C, which indicates that it originates from the dopant. No fragments with a mass above 60 amu are detected. Also no traces from ethylacetate [14], which was used as solvent for GAP, was detected. This is different to PVN and PVC where strong signals were assigned to the solvent. One possible reason is the production process of the films, i.e. GAP is cross-linked from a 70 wt-% polymer solution, whereas PVN and PVC are solvent cast from 10 to 20 wt-% solutions [8]. This results in less solvent trapped in the polymer after the production process in the case of GAP films.

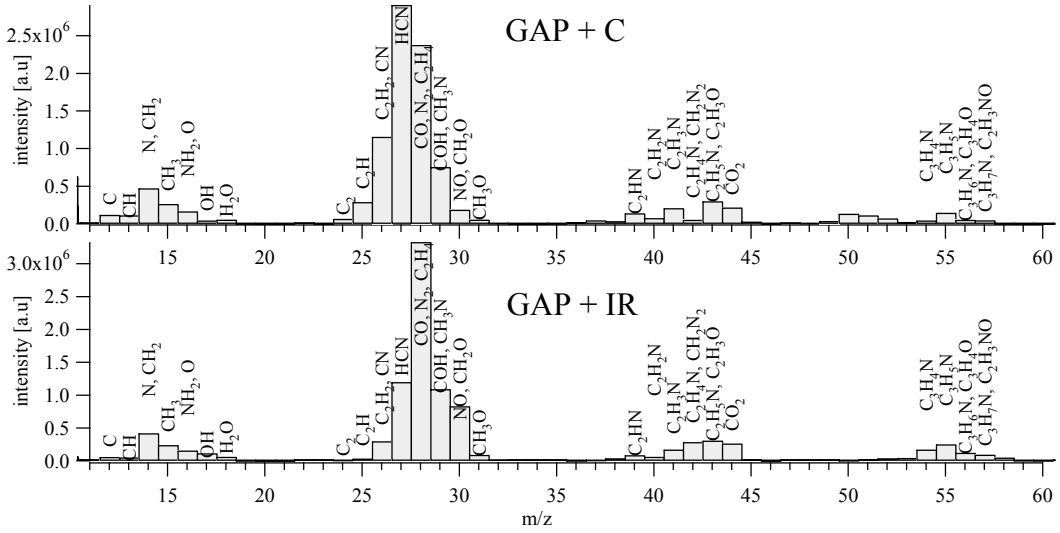

Figure 7: Mass spectrum of the neutral fragments from GAP+C (top) and GAP+IR (bottom) after irradiation with 10 J cm^{-2} at 1064 nm.

The same signals for GAP with both dopants have been detected in the positive ion spectra (shown in Fig. 8). The strongest signal in the case of the carbon doped GAP could be assigned to Na^+. Also Cl has been detected which indicates a contamination of either the polymer or the dopant by NaCl. A much stronger signal for Na^+ has been detected for all carbon doped polymers compared to the IR-doped GAP. For the carbon doped polymers a surface contamination by careless handling can be excluded, as such a strong signal for Na+ would not be caused by a small deposition on the surface, suggesting that the Na is a contamination in the carbon dopant. The strongest peak for GAP+IR can be assigned to C^+. This indicates a higher fragmentation of the polymer backbone for the IR-dye doped

GAP, which is consistent with the shadowgraphy measurements reported by Urech et al. [8]. In the ablation plume of the IR-dye doped GAP no larger fragments were visible in the shadowgraphy measurements, whereas for GAP+C a large amount of heavy fragments were detected.

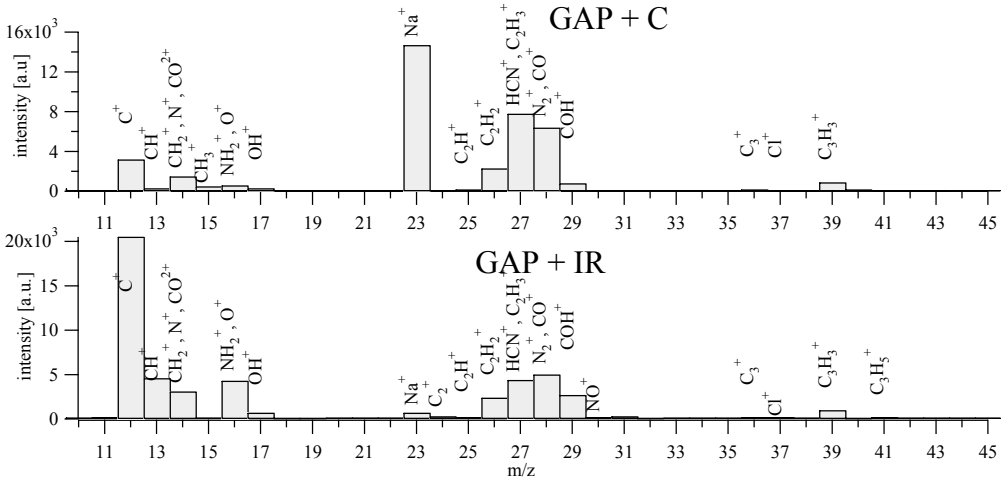

Figure 8: Mass spectrum of the positive charged ion fragments from GAP+C (top) and GAP+IR (bottom) after irradiation with 13.7 J cm^{-2} at 1064 nm

Other fragments from the polymer are again N_2^+ and HCN^+ and fragments from the polymer backbone. As observed in the neutral spectra, the intensities between N_2^+ and HCN^+ are switched for the two dopants. This indicates a slightly different decomposition mechanisms for GAP with the two absorbers. For GAP+C a decomposition into HCN^+ is favored, whereas for GAP+IR a decomposition into N_2^+ and NH_2^+ is dominant and less HCN^+ is produced. This is also supported by the stronger NH_2^+ signal for the IR dye doped samples (see Fig. 8).
A possible decomposition pathway for GAP with both dopants is shown in Fig. 9. In a first step N_2 is released from the azide group. In a second step either NH_2 or HCN are removed, before the decomposition of the polymer backbone starts [15-17].

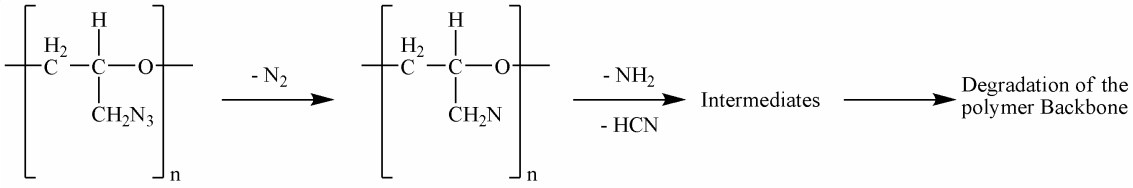

Figure 9: Proposed decomposition pathway for GAP+C and GAP+IR for irradiation with 1064 nm.

The kinetic energies of C^+ for GAP+C and GAP+IR for different irradiation fluences are shown in Fig. 10.
For GAP+C (left) two distributions can be distinguished. A first maximum is observed around 10 eV, while the second much stronger and broader distribution is located at ~55 eV. With increasing fluence, more ions are detected, but the ratio between the two peaks and the distribution does not change as observed for PVC+C. The maximum intensity of the second peak is also similar for both polymers.

In the case of GAP+IR (Fig. 10, right) a strong signal at ~10 eV is observed at the lowest fluence of 7 J cm^{-2}. The intensity of this peak remains constant for all fluences. A second peak around 55 eV shows a strong dependence on the irradiation fluence. At 7 J cm^{-2}, the maximum is lower than for the first peak, at 14 J cm^{-2} the same intensity for both peaks is observed and at 23 J cm-2, the second peak is stronger than the first peak. The maximal intensity of the peak at 55 eV is similar for GAP with both dopants at the highest fluence.

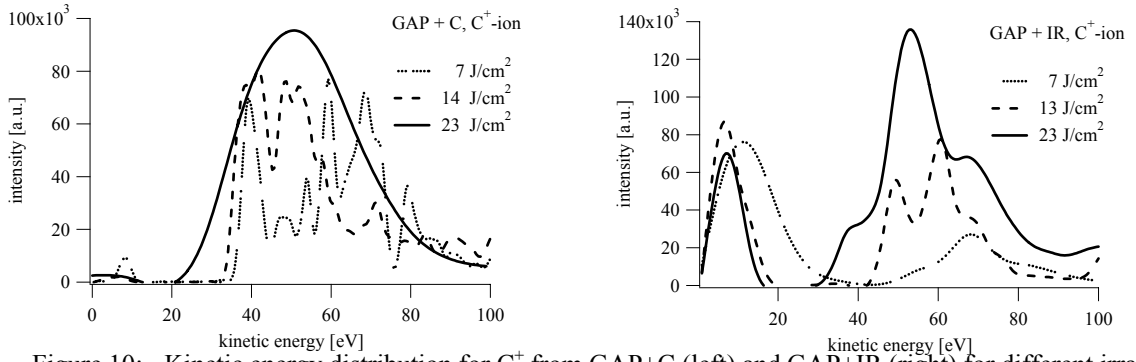

Figure 10: Kinetic energy distribution for C^+ from GAP+C (left) and GAP+IR (right) for different irradiation fluences with 1064 nm nm

For GAP with both dopants the same fragments were observed, but with different intensities. The IR-doped GAP showed a higher sensitivity to the irradiation fluence. The backbone of the IR-doped GAP decomposes into smaller fragments. The kinetic energy has also a strong dependence on the irradiation fluence. This might be caused by the different distribution of the two dopants in the polymer. The IR-dye is distributed on a molecular level and the energy is therefore absorbed more uniformly than in the case of the carbon doped GAP, where carbon agglomerates of up 20 µm may be present [10]. These agglomerates absorb the laser light and form local hotspots. Polymer in the close surrounding of these hotspots then is exposed too much higher temperatures than the IR doped GAP at the same fluence. In the case of the carbon doped polymer, less polymer is therefore decomposed, but the ionic fragments have an already higher energy at lower fluences than in the case of IR-dye doped GAP. Only at the highest irradiation fluence, the same intensity could be observed for ions from both GAP/dopant-systems.

3.1.3. PVN doped with carbon nanoparticles

The most intense peak in the neutral mass spectra for PVN+C is 28 (Fig. 11), which can be assigned to CO, as the formation of N_2 in the plasma plume is not very likely. No fragments at higher masses, such as 89 amu (monomer mass) or O_2 were detected.

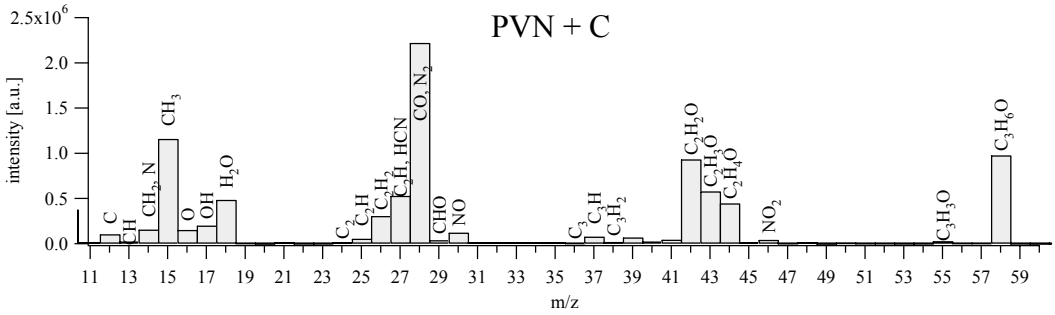

Figure 11: Mass spectrum of the neutral fragments from PVN+C after irradiation with 10 J cm^{-2} at 1064 nm.

The strong signals at mass 58 and 43 can be assigned to acetone [14], which is the solvent used to cast the films from a 20 wt-% polymer solution [8]. On possible origin of solvent remaining in the polymer film is due to the fast evaporation of the solvent from the cast layer which results in the formation of a dense surface layer. Solvent below this layer is then trapped in the polymer film and cannot be removed in the normal vacuum drying procedure [18].
The strongest peaks in the positive ion spectra (shown in Fig. 12) can be assigned to CO^+, C^+ and NO^+. Again no peaks were detected for O_2^+ and NO_2^+, which could be possible fragments in the decomposition of PVN, similarly to the decomposition of inorganic nitrates [19].

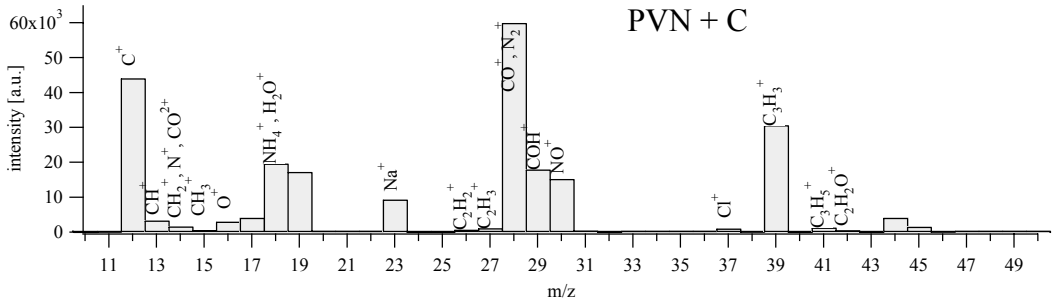

Figure 12: Mass spectrum of the positive charged ion fragments from PVN+C after irradiation with 23 J cm^{-2} at 1064 nm

The kinetic energy distribution for C^+ (left) and N^+ (right) from PVN+C are shown in Fig. 13. For both species the same behavior can be observed as in the case of GAP+C. A weak peak is detected around 10 eV, and a stronger much broader peak is situated at ~40 to 50 eV. The N^+-ions show a slightly higher sensitivity to the irradiation fluence. The C^+-ions

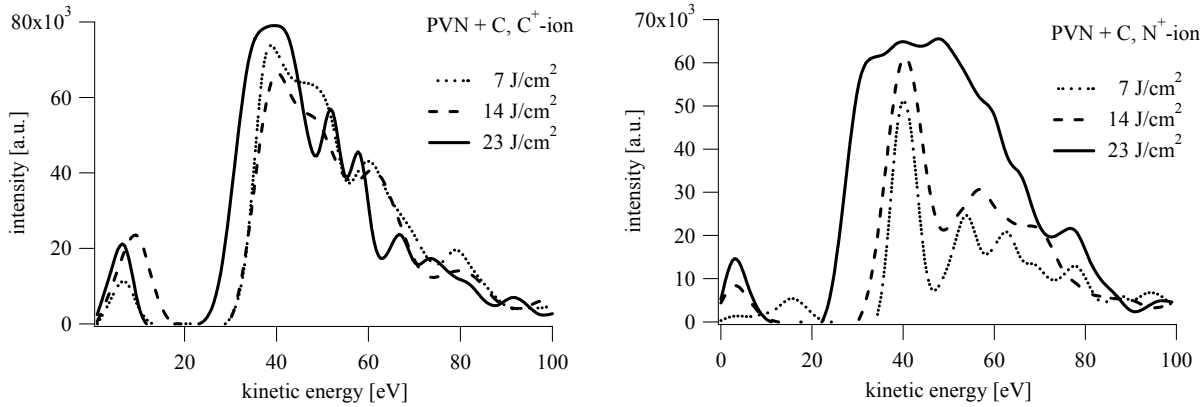

Figure 13: Kinetic energy distribution for C^+ (left) and N^+ (right)PVN+C for different irradiation fluences with 1064 nm.

are not influenced by the fluence. Neither the position nor the intensity of the peaks are changed with increasing energy. For N^+-ions, the irradiation fluence increases the amount of ions, but the kinetic energy distribution remains more or less constant.
Also the maximal of the strong peaks at 50 eV is in the same range as for GAP+C and PVC+C.

3.1.4. Summary of the mass spectrometry measurements

The kinetic energy spectra for C^+ of both energetic polymers show a small peak at 10 eV and several peaks between 30-80 eV. For GAP+C an increase of the signal intensity with increasing fluence is observed, whereas no influence of the fluence could be observed for PVN+C. N^+ ions from PVN+C show a stronger sensitivity to the fluence, e.g. the intensity of the peak between 30 and 80 eV increases, whereas the peak at 10 eV stays constant. This indicates that the additional energy delivered at higher fluences is mainly "used" to produce more ions in the higher energy range.
This is not observed for PVC+C, where the intensity of all C^+ ions is increased, regardless of their energy.
A high amount of C^+ ions with a energy of 10 eV is observed for GAP+IR, but the intensity of this peak does not increase with increasing laser fluence. The higher energetic C^+ ions show again a much stronger dependence on the laser fluence, e.g. a strong increase in the intensity with increasing laser fluence.

3.2. Thrust measurements

The thrust measurements revealed the highest I_{sp} for PVN + C (2320 s), whereas the other polymers showed much lower values (200 to 650 s) (dark grey in Fig. 14). A correlation of the specific impulse with material properties is not yet established.

The highest values for C_m were obtained for GAP + IR (2000 µN/W), followed by GAP + C, PVN + C and PVC + C (1170 to 120 µN/W) (light gray in Fig. 14). The high C_m value for the IR-doped polymer indicates a high transformation of polymer into the gaseous state, as also observed in the shadowgraphy and SEM measurements [8].

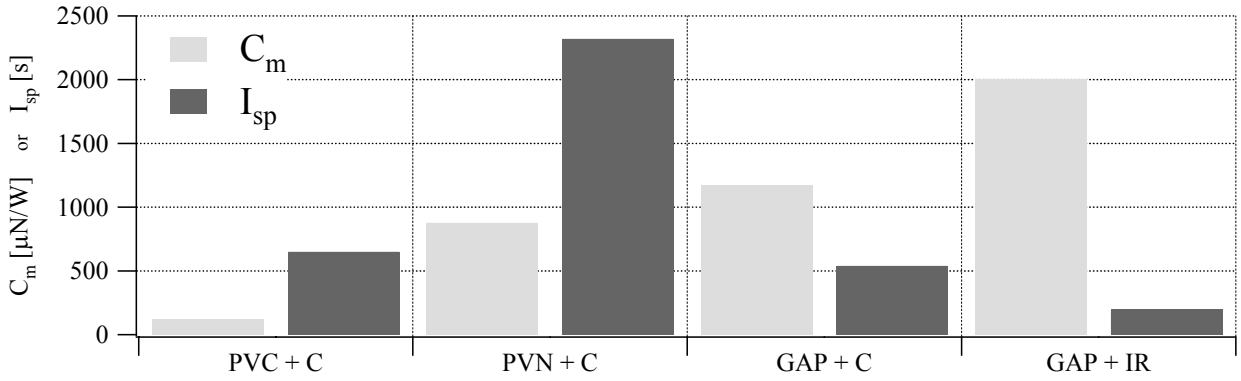

Figure 14: Thrust measurements

4. CONCLUSIONS

A higher degree of fragmentation has been detected for the energetic polymers GAP and PVN compared to PVC. For all polymers the expected signals have been detected. For the energetic polymers mainly nitrogen containing groups, i.e. HCN and N_2 for GAP and NO for PVN, and fragments from the polymer backbone were detected. The main decomposition products for PVC were also fragments from the polymer backbone and HCl.

A strong signal from the solvent used in the polymer film production was detected for PVN and PVC. Both polymers were solvent cast from dilute (10 to 20 %) polymer solution. In the mass spectra of GAP with both dopants no signal could be assigned to the solvent. The main difference to PVN and PVC is that GAP is cross-linked from a 70 % polymer solution, and less solvent is present throughout the whole process. This solvent can influence the thrust achieved with the polymers, as it acts as "inert" material during the ablation progress. A slow evaporation over time may also alter the mechanical properties and cause problems in the thruster mechanics.

In the carbon doped polymers a strong signal of Na was detected. The signal is too strong to be caused by a contamination of the polymer surface. The carbon is therefore the most probable source of the NaCl contamination, as much less sodium is detected for GAP+IR.

A higher fragmentation was also detected for GAP+IR compared to GAP+C. This is consistent with the shadowgraphy measurements, where no larger fragments were detected in the ablation plume of GAP+IR.

The kinetic energies of selected positively charged ions show a similar behavior for all carbon doped polymers. A peak at 10 eV and several peaks between 30-80 eV can be observed for C^+ of both energetic polymers. The laser fluence does not influence the intensity of the peaks in the case of PVN+C. For GAP+C an increase of the signal intensity has been observed with increasing fluence. The same peaks are also observed for the N^+ ions from PVN+C, but here only the amount of higher energetic ions is increased with the fluence. The same behavior has also been detected for the C^+ of GAP+IR. For PVC+C no selective increase of the signal intensity is observed.

For energetic polymers, a transformation of induced laser energy to measured thrust of more than 100% was observed. This indicates that energy gained from decomposing the polymer can be transferred into thrust and that the ablation mechanism plays only a minor role. The decomposition of the energetic polymers into smaller fragments than in the case of PVC corresponds well to the higher momentum coupling coefficient of the energetic polymers, which indicates that more thrust can be gained from a chosen incident laser power.

Until now, no correlation between the kinetic energies of the ablation products and the specific impulse could be established. Also no relation between irradiation fluence, kinetic energy the ablated products and thrust has been detected.

These experiments demonstrate that the main demand on polymers as fuel for the μ-LPT is a high decomposition enthalpy. Furthermore a high transition rate of the polymer into gaseous products or small fragments is favorable, as more energy can be gained.

ACKNOWLEDGEMENTS

The authors would like to thank M. Nagel (EMPA, Dübendorf, Switzerland) and Nitro Chemie Wimmis for supplying some of the materials.
Effort sponsored by the Air Force Office of Scientific Research, Air Force Material Command, USAF, under grant number FA8655-03-1-3058. The U.S. Government is authorized to reproduce and distribute reprints for Government purpose notwithstanding any copyright notation thereon.

REFERENCES

1. C. Phipps, J. Luke, and T. Lippert, *Laser ablation of organic coatings as a basis for micropropulsion.* Thin Solid Films, 2004. **453-454**: p. 573-583.
2. C.R. Phipps, J.R. Luke, G.G. McDuff, and T. Lippert, *Laser-driven micro-rocket.* Applied Physics a-Materials Science & Processing, 2003. **77**(2): p. 193-201.
3. C. Phipps, J. Luke, T. Lippert, M. Hauer, and A. Wokaun, *Micropropulsion using a laser ablation jet.* Journal Of Propulsion And Power, 2004. **20**(6): p. 1000-1011.
4. T. Lippert, C. David, M. Hauer, T. Masubuchi, H. Masuhara, K. Nomura, O. Nuyken, C. Phipps, J. Robert, T. Tada, K. Tomita, and A. Wokaun, *Novel applications for laser ablation of photopolymers.* Applied Surface Science, 2002. **186**(1-4): p. 14-23.
5. T. Lippert, M. Hauer, C.R. Phipps, and A. Wokaun, *Fundamentals and applications of polymers designed for laser ablation.* Applied Physics a-Materials Science & Processing, 2003. **77**(2): p. 259-264.
6. C. Phipps, J. Luke, G.G. McDuff, and T. Lippert, eds. *Laser Ablation Powered Mini-Thrusters*. High-Power Laser Ablation IV, Proceedings of the SPIE, ed. C. Phipps. Vol. 4760. 2002, SPIE.
7. C. Phipps and J. Luke, *Diode laser-driven microthrusters: A new departure for micropropulsion.* AIAA Journal, 2002. **40**(2): p. 310-318.
8. L. Urech, M. Hauer, T. Lippert, C.R. Phipps, E. Schmid, A. Wokaun, and I. Wysong, *Designed polymers for laser-based microthrusters - correlation of thrust with material, plasma, and shockwave properties.* Proceedings of the SPIE, 2004. **5448**: p. 52-64.
9. D.S. Moore and S.D. McGrane, *Comparative infrared and Raman spectroscopy of energetic polymers.* Journal of Molecular Structure, 2003. **661**: p. 561-566.
10. R.P. Richner, *Entwicklung neuartig gebundener Kohlenstoffmaterialien für elektrische Doppelschichtkondensatorelektroden*. 2001, ETH: Zürich.
11. M.H. Fisch and R. Bacaloglu, *Kinetics and mechanism of the thermal degradation of poly(vinyl chloride).* Journal of Vinyl & Additive Technology, 1995. **1**(4): p. 233-240.
12. R. Bacaloglu and M.H. Fisch, *Reaction mechanism of poly(vinyl chloride) degradation. Molecular orbital calculations.* Journal of Vinyl & Additive Technology, 1995. **1**(4): p. 241-249.
13. I.C. McNeill, L. Memetea, and W.J. Cole, *A Study of the Products of Pvc Thermal-Degradation.* Polymer Degradation and Stability, 1995. **49**(1): p. 181-191.
14. M. Hesse, H. Meier, and B. Zeeh, *Spektroskopische Methoden in der organischen Chemie*. 5. ed. 1995, Stuttgart: Georg Thieme Verlag.
15. Y. Haas, Y. Ben-Eliahu, and S. Welner, *Pulsed laser induced decomposition of energetic polymers: Comparison of ultraviolet (355 nm) and infrared (9.3 mu m) initiation.* Propellants Explosives Pyrotechnics, 1996. **21**(5): p. 258-265.
16. C.J. Tang, Y.J. Lee, and T.A. Litzinger, *Simultaneous temperature and species measurements of the Glycidyl Azide Polymer (GAP) propellant during laser-induced decomposition.* Combustion And Flame, 1999. **117**(1-2): p. 244-256.
17. O.P. Korobeinichev, L.V. Kuibida, E.N. Volkov, and A.G. Shmakov, *Mass spectrometric study of combustion and thermal decomposition of GAP.* Combustion And Flame, 2002. **129**(1-2): p. 136-150.
18. T. Lippert, R.L. Webb, S.C. Langford, and J.T. Dickinson, *Dopant induced ablation of poly(methyl methacrylate) at 308 nm.* Journal Of Applied Physics, 1999. **85**(3): p. 1838-1847.
19. J.J. Shin, D.R. Ermer, S.C. Langford, and J.T. Dickinson, *The role of photoelectronic processes in the formation of a fluorescent plume by 248-nm laser irradiation of single crystal $NaNO_3$.* Applied Physics A-Materials Science & Processing, 1997. **64**(1): p. 7-17.